JACS
JOURNAL OF THE AMERICAN CHEMICAL SOCIETY
Article
pubs.acs.org/JACS

Genetically Encoded Copper(I) Reporters with Improved Response for Use in Imaging

Jun Liu,[†] Jason Karpus,[‡] Seraphine V. Wegner,[‡,#] Peng R. Chen,*[,†,§] and Chuan He*[,†,‡]

[†]Beijing National Laboratory for Molecular Sciences, Synthetic and Functional Biomolecules Center, College of Chemistry and Molecular Engineering, Peking University, Beijing 100871, China

[‡]Department of Chemistry and Institute for Biophysical Dynamics, The University of Chicago, 929 East 57th Street, Chicago, Illinois 60637, United States

[§]Peking-Tsinghua Center for Life Sciences, Beijing 100871, China

Supporting Information

ABSTRACT: Copper represents one of the most important biological metal ions due to its role as a catalytic cofactor in a multitude of proteins. However, an excess of copper is highly toxic. Thus, copper is heavily regulated, and copper homeostasis is controlled by many metalloregulatory proteins in various organisms. Here we report a genetically encoded copper(I) probe capable of monitoring copper fluctuations inside living cells. We insert the copper regulatory protein Ace1 into a yellow fluorescent protein, which selectively binds copper(I) and generates improved copper(I) probes.

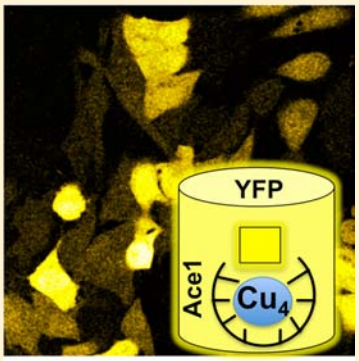

INTRODUCTION

Due to its reactivity with oxygen and importance in cellular redox reactions, copper is one of the most important catalytic metal cofactors.[1−3] The total concentration of copper can approach levels of 10−100 μM in organisms such as yeast, a relatively high level in comparison to other first-row transition metal ions. However, the level of labile copper is relatively low due to the capacity of many proteins and other ligands to bind copper with high affinity.[2] In *Escherichia coli*, the concentration of labile copper is tightly regulated by the regulatory protein CueR and has been reported to be ∼10^{-21} M.[4] The concentration of free copper in yeast is also low and buffered to be ∼10^{-18} M.[5] This low level of labile copper is crucial physiologically, as elevated copper levels are highly toxic.[6] Furthermore, the misregulation of copper concentration inside the human brain leads to neurodegeneration, cardiovascular disorders, and Menkes and Wilson's diseases.[7−9] As such, monitoring the fluctuations of copper inside living cells is important to research on copper homeostasis, which in turn would have significant implications in human health.

Developing metal ion sensors has proved challenging, but a variety of techniques have emerged that allow for the study of a myriad of different metal ions.[10] Due to the high affinity of certain metalloregulatory proteins for copper, it has been difficult to measure and monitor changes in the concentration of copper(I) inside cells. A number of small-molecule fluorescent sensors for copper(I) have been developed,[11−22] but most of these small-molecule probes lack the necessary binding affinity for copper(I) to compete with other chelators in cytosal. Additionally, copper binding selectivity, water insolubility, cytotoxicity, and difficulties in either entering the cell or targeting specific organelles are potential problems associated with synthetic probes. As such, it could be advantageous to adopt genetically encoded probes as alternative or complementary approaches.

Genetically encoded reporters have been used in the past with great success. Protein-based genetically encoded sensors for both calcium[23−25] and zinc[26−29] have been reported, and their utility for monitoring their desired metal ion *in vivo* is well established. Based on these previous successes, our laboratory was able to engineer the first genetically encoded copper(I) sensor, Amt1-FRET.[30] Our construct utilized the copper binding domain of Amt1, a copper-dependent regulator in the yeast *Candida glarate*,[31,32] and subcloned it between a cyan fluorescent protein (CFP) and a yellow fluorescent protein (YFP). Despite its superb selectivity for copper and the success the probe had in imaging copper in living cells, this construct was not without its limitations. The design made it difficult to vary the copper binding affinity of the probe. Additionally, the maximum FRET response was only 15%, below the response levels of the most efficacious probes. Therefore, generating a genetically encoded copper(I) sensor with an increased

Received: November 1, 2012
Published: January 29, 2013

   dx.doi.org/10.1021/ja3106779 | *J. Am. Chem. Soc.* 2013, 135, 3144−3149

response and an attenuated binding affinity is highly desirable for effective monitoring of copper(I) *in vivo*.

EXPERIMENTAL SECTION

Expression and Purification of Proteins. The metal binding domain of Ace1 (36−100) was cloned between residues 145 and 146 of eYFP using *Sph*I and *Sac*I in a pet28a plasmid. Additional subcloning was performed to add different numbers of GGS linkers between residue 145 on EYFP and Ace1 in our fusion protein. Probes are referred to as YAG*n*, for YFP-Ace1 with *n* GGS linkers. These resulting plasmids were transformed into BL21star(DE3). To express our constructs, single colonies were used to inoculate a 10 mL starter culture overnight, and the starter cultures were subsequently used to inoculate 1 L of autoclaved LB medium containing 50 mg of ampicillin. The cells were grown at 37 °C, 250 rpm to OD_{600} = 0.6, at which time the temperature was reduced to 16 °C. After 30 min, protein expression was induced with 0.5 mM IPTG and 1.4 mM $CuSO_4$, and expression was allowed to continue overnight. Cells were harvested at 4 °C by centrifugation at 6000 rpm for 8 min. All subsequent steps were performed at 4 °C.

The pellet was suspended in 20 mL of buffer A (10 mM Tris-HCl [pH 7.4], 300 mM NaCl, 4 mM DTT) and 10 mM PMSF. The cells were lysed by sonication and centrifuged at 12 000 rpm for 25 min. The supernatant was filtered through a 0.45 μm filter and applied to a Ni-NTA column. The column was washed with 5% buffer B (10 mM Tris-HCl [pH 7.4], 500 mM imidazole, 300 mM NaCl, 4 mM DTT) and eluted with a linear gradient from 5% to 100% buffer B over 40 mL. Peak fractions were pooled and kept at 4 °C. To obtain apo-YAG*n*, 10 mM NaCN was added to the purified proteins, and after a brief incubation period the proteins were run through a desalting column using buffer A containing 8 mM DTT.

Fluorescence Measurements. All fluorescence measurements were carried out at room temperature on a Varian Cary Eclipse fluorescence spectrophotometer. The samples were excited at 496 nm, the excitation and emission slit widths were set to 5 nm, and the emission spectrum was scanned from 505 to 600 nm at 120 nm/min.

The titration and selectivity measurements were performed in a buffer containing 100 mM HEPES (pH 7.0), 300 mM NaCl, and 4 mM DTT, except for measurements with Ag^+ and Pb^{2+}, where 100 mM HEPES (pH 7.0), 300 mM $NaNO_3$, and 4 mM DTT buffer were used instead. Tetrakis(acetonitrile)copper(I) hexafluorophosphate dissolved in acetonitrile at 100 μM concentration was used as the copper(I) source in all measurements. For the other metals, 100 μM stock solutions were prepared from the following salts with purity >99%: $AgNO_3$, $ZnCl_2$, $MgCl_2$, $CaCl_2$, $Cr(NO_3)$, $MnCl_2$, $Fe(NH_4)_2SO_4$, $CoCl_2{\cdot}6H_2O$, $NiCl_2{\cdot}6H_2O$, $CdCl_2$, $Hg(NO_3)_2$, and $Pb(NO_3)_2$. For the titration curves of YFP-Ace1, a 0−12 μM concentration of each metal was added to a solution of 1 μM apo-YAG*n* protein, and the response at 527 nm was taken as a measure of turn-on efficiency. For the selectivity measurement of YAG*n*, a 5 μM concentration of each metal was added to 1 μM apo-YFP-Ace1, and the response to the metal was measured. Then, 5 μM Cu^+ was added to the same solution, and the response was recorded again. To test potential interference from common anions in biological systems, the response was monitored for both apo-YAG*n* and Cu-YAG*n* in the presence of 5 μM concentrations of the following salts: ammonium chloride, sodium acetate, sodium citrate, sodium bicarbonate, sodium sulfate, and sodium phosphate. All experiments were repeated for each of our probes.

Determination of Cu^+ Binding Constant. For the K_d measurement of YAG*n* with Cu^+, Cu^+/CN^- buffers were used to obtain free Cu^+ concentrations ranging from 8.29×10^{-21} to 8.61×10^{-16} M. The concentration of free Cu^+ was calculated using the known Cu^+ binding constants to cyanide and the proton association constant (K_a) for CN^- obtained from the NIST Critical Stability Constants of Metal Complexes, the values of which are shown below.

$$H^+ + CN^- \leftrightarrow HCN \qquad \log K_a = 9.04$$

$$Cu^+ + 2CN^- \leftrightarrow Cu(CN)_2^- \qquad \log \beta 2Cu = 21.7$$

$$Cu^+ + 3CN^- \leftrightarrow Cu(CN)_3^{2-} \qquad \log \beta 3Cu = 26.8$$

$$Cu^+ + 4CN^- \leftrightarrow Cu(CN)_4^{3-} \qquad \log \beta 4Cu = 27.9$$

Free copper concentration was calculated using the program HySS2006, with total Cu^+ concentrations in the buffer ranging from 3.8×10^{-5} to 1.0×10^{-3} M and CN^- concentrations ranging from 2.5×10^{-4} to 2.0×10^{-2} M. The levels of the individual components of these buffers were kept as follows: CN^- (0.25−20 mM) > Cu^+ (38 μM−1 mM) ≫ YAG*n* probe (2.5 μM). The metal buffering capacity of cyanide was used to precisely control free copper(I) concentrations, but the total level of copper(I) was always kept much higher than the concentration of our reporter. YAG*n* concentration was maintained at 2.5 μM in 100 mM HEPES (pH 7.0) and 100 mM NaCl, and the response was measured for each copper(I) buffer prepared. The response of YAG*n* toward the free copper(I) concentration in the buffer was plotted, and the binding curve was fitted to the Hill equation using Origin 8.

UV−Vis Measurements. Purified YAG*n* was treated with 10 mM CN^- and run through the desalting column using the previously described buffer. The UV−vis absorption spectrum for apo-YFP-Ace1 was measured in 100 mM HEPES (pH 7.0), 300 mM NaCl, and 8 mM DTT.

Imaging and Cell Culturing. HeLa cells were maintained at 37 °C under 5% CO_2 in DMEM supplemented with 10% FBS. For the expression of YAG2, HeLa cells were seeded overnight into 35 mm glass-bottom Petri dishes (MatTek) to obtain 70−90% confluency. The following day, the cells were transfected with pcDNA4.0(+) carrying YAG2 using Lipofectamine LTX (Invitrogen) according to the manufacturer's protocol. After a 24−48 h expression period, the cells were used for imaging. Imaging was done on a Leica TCS SP2 AOBS laser scanning confocal microscope equipped with a 63× oil objective. Images were collected using the included software and analyzed with ImageJ 1.38x (Rasband, W.S., ImageJ, U.S. National Institutes of Health, Bethesda, MD, 1997−2007, http://rsb.info.nih.gov/ij/). Images of the YAG2-transfected HeLa cells were obtained by exciting at 496 nm. Both YFP excitation and bright-field images were obtained. Prior to data collection, the medium was changed, and cells were put into 1.5 mL of HBSS buffer. Images were collected prior to addition of any copper, and then 50 μM $CuSO_4$ was added to the cells. Images were collected every 30 s for a 5-min period. Subsequently, a 1 mM concentration of the copper(I) ligand, neocuproine, was added to the cells, and the response was observed every minute for a 20-min period. The response to other metals was also tested by adding 50 μM $ZnCl_2$ and 1 mM EGTA and monitoring the fluorescence over a similar time period.

Fluorescence-Activated Cell Sorting Experiments. HeLa cells were transiently transfected with a YAG*n* probe using the vector pcDNA4.0. After 24 h, cells were harvested by trypsinization and washed twice with PBS. Next, 500 μM $CuSO_4$ and 500 μM neocuproine were added to different suspensions 30 min before initiation of the flow. The 488-nm lasers of a CyAn ADP flow cytometer (DakoCytomation) were used for excitation, and 530/540-nm filters were used for emission. Data were analyzed using Summit software (DakoCytomation).

RESULTS AND DISCUSSION

Construction of a New Series of Cu^+ Reporters. To improve upon our initial design, we utilized copper(I)-dependent transcriptional regulatory proteins similar to those we used previously.[30] Ace1, a copper(I) regulatory protein homologous to Amt1 in *Saccharomyces cerevisiae*,[32,33] was used in this study. Ace1 has three distinct domains: a zinc finger domain, a copper(I) binding domain, and a transactivation domain (Figure S1). Upon exposure to copper(I), the eight

dx.doi.org/10.1021/ja3106779 | J. Am. Chem. Soc. 2013, 135, 3144−3149

cysteines in the copper(I) binding domain form a tetracopper-(I) cluster.[34,35] The reversible formation of this copper(I) cluster leads to a conformation change which helps to modulate the binding affinity of Ace1 with DNA. In this study, the copper(I) binding domain of Ace1 was inserted between the residues Y145 and N146 of YFP to make the copper(I) fluorescent reporter YFP-Ace1. The copper(I) binding domain was intentionally inserted near the fluorophore of YFP in order to maximize the effects of copper(I) binding. The conformation change that occurs when Ace1 binds copper(I) will cause a change in the local environment near the fluorophore of YFP, which in turn will alter its fluorescent properties. Subsequently, we altered our initial construct to create a series of probes with flexible peptide linkers consisting of GGS repeats of different lengths after the copper(I) binding domain of Ace1 and before the N146 residue of the YFP to attenuate the probe's binding affinity to copper(I). This strategy has proven to be a useful, modular approach to obtain reporters with different binding affinities that could be applied in unique cellular environments.[36] In this study, we constructed five reporters with different numbers of GGS linkers (0–4) (Figure 1). The probes were named YAG*n*, where *n* corresponds to the number of GGS linkers inserted into the probe.

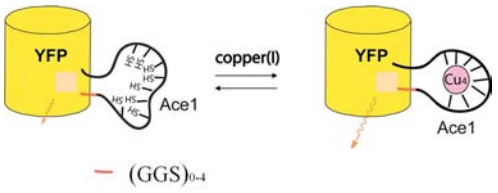

Figure 1. The design of a series of new fluorescent Cu^+ reporters, YFP-Ace1, with varying linker lengths. The copper(I) binding domain of Ace1 was cloned between residues Y145 and H146 of YFP, putting it in close proximity to the fluorophore. Different lengths of GGS linkers were added to tune the binding affinity and response level. The addition of free Cu^+ causes Ace1 to bind copper as a tetracopper cluster, resulting in a conformational change of the binding region. This conformational change causes a change in the local environment of the fluorophore, which should in turn change the fluorescent response.

***In Vitro* Characterization of YAG*n* Probes.** Each of our YFP-Ace1 constructs was expressed in *E. coli* in the presence of 1 mM $CuSO_4$ to ensure proper folding of the copper binding region. All constructs were purified via fast protein liquid chromatography (FPLC) to produce the Cu^+-bound form of the probes (Figure S2). Incubation with cyanide was sufficient to regenerate the apo form, as determined by monitoring the copper(I) thiolate charge-transfer band using UV–vis spectroscopy (Figure S3).[32] For all of our probes, the fluorescent spectra of both apo and copper(I)-bound forms were obtained by exciting the YFP at 496 nm and recording the subsequent emission at 515 nm. The addition of Cu^+ caused a significant increase in the emission for all of the YAG*n* probes, most notably at physiologically relevant pH (Figure S4). Complete saturation of YAG0 with Cu^+ generated a nearly 40% increase in fluorescence emission, with similar increases observed for the other probes (Table 1, Figures S5 and S6). The addition of Cu^+ to one of the probes, YAG2 (selected due to its superior response inside cells), resulted in a nearly 25% increase in emission when compared to the apo form of the protein (Figure 2A). As expected, the fluorescent measurements

Table 1. Response to Cu^+ with Varying Linker Lengths

GGS repeats (*n*)	K_d (M)	response (%)
0	$(8.2 \pm 1.2) \times 10^{-18}$	38
1	$(2.0 \pm 0.8) \times 10^{-18}$	35
2	$(1.2 \pm 1.0) \times 10^{-18}$	30
3	$(4.6 \pm 1.2) \times 10^{-19}$	25
4	$(3.3 \pm 0.9) \times 10^{-19}$	25

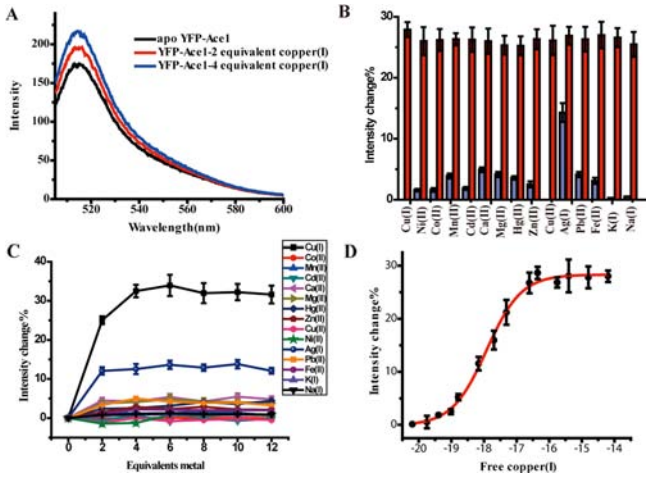

Figure 2. Fluorescent response of YAG2. (A) Titration of YAG2 with increasing amounts of Cu^+ under 4 mM DTT. (B) Selectivity of YAG2 toward Cu^+. The probe (1 μM) was incubated with 5 μM of various metals prior to the addition of 5 μM Cu^+. Recovery of the fluorescence with Cu^+ is shown as the second bar for each metal ion. (C) Fluorescence response of YAG2 after the addition of various equivalents of biologically relevant metal ions. (D) Specificity of YAG2. The binding curve for Cu^+ was determined by using increasing amounts of free Cu^+.

indicate that our YAG*n* probes are capable of binding 4 equiv of copper(I). Interestingly, modifying the number of GGS repeats in the linker of the probe altered the level of response, which varied between ~25 and 40%, depending on the length of linker used. Shorter linkers seem to be more effective in inducing a more significant conformational change nearer to the fluorophore, leading to a greater change in the localized environment and an increased response.

Varying the linker length also modulated the nature of the response. Shorter linker lengths, as used in YAG0 or YAG1, generated a ratiometric response (Figure 3A,B), while longer linker lengths were incapable of doing so. Monitoring the emission of the probe when excited at either 440 or 496 nm gave significantly different fluorescent spectra. For either YAG0 or YAG1, addition of Cu^+ caused decreased emission at 515 nm upon excitation at 440 nm. In comparison, the response at 515 nm increased under the same conditions if excitation occurred at 496 nm (Figure 3A,B). Shorter linker lengths generated a more significant ratiometric response, with the ratiometric nature of YAG0 being more pronounced than that of YAG1. YAG2 lost the ratiometric response entirely, as excitation at 440 nm failed to change the emission, giving the probe more of a turn-on/turn-off response instead (Figure 3C).

To determine the selectivity of our probes, we tested the response of each probe to a variety of biologically relevant metal ions (Figures 2B, S5C, and S6C). Using YAG2 as an example, besides Cu^+, only Ag^+ induced a response over 5%. All other metal ions, including biologically relevant ones like Ca^{2+},

dx.doi.org/10.1021/ja3106779 | J. Am. Chem. Soc. 2013, 135, 3144–3149

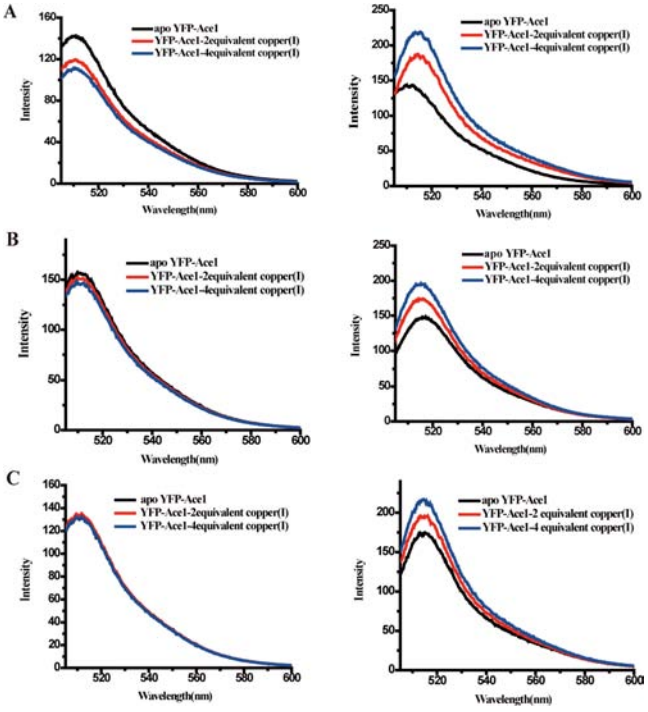

Figure 3. Ratiometric properties of the YFP-Ace1 probes with various linkers. Fluorescent responses of (A) YAG0 when excited at 440 (left) and 494 nm (right) when supplemented with additional copper(I). Responses are also shown for (B) YAG1 and (C) YAG2. These responses indicate a significant ratiometric response for YFP-Ace1, a moderate ratiometric response for YAG1, and no ratiometric response for YAG2.

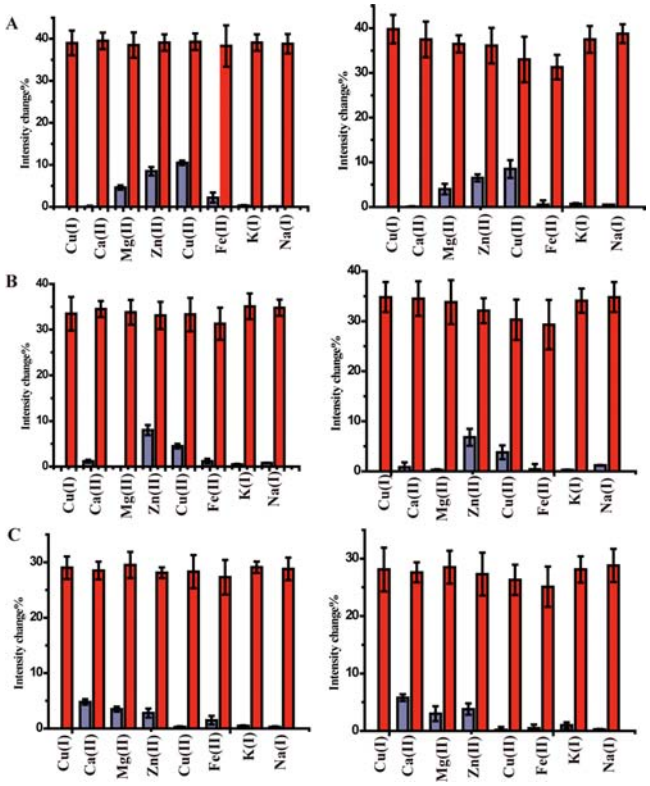

Figure 4. Selectivity of the YAG*n* series of probes. A 1 μM concentration of probe was incubated with either 10 (left) or 50 μM (right) concentrations of various metals before the solution was supplemented with 5 μM copper(I) for (A) YAG0, (B) YAG1, and (C) YAG2. Recovery of the fluorescence with Cu^+ is shown as the second bar for each metal ion.

Mg^{2+}, Zn^{2+}, and Cu^{2+}, either failed to bind the reporter or generated only a minimal response. To further assess the specificity of the YAG probes for Cu^+, a competition assay was performed to ensure they could respond to Cu^+ even in the presence of an excess of other metal ions. The fluorescence response was first recorded after addition of 5 equiv of various other metal ions to the apo version of the probe. Subsequently, 5 equiv of Cu^+ was added, and the fluorescent response was recorded again. Addition of Cu^+ was always successful in recovering the maximum response, regardless of the presence of other metals, for YAG2 (Figure 2C). Similar results were also observed for our other probes (Figures S5B and S6B). Furthermore, even elevated concentrations of other metal ions (as high as 50 μM) were unable to disrupt copper(I) recognition (Figure 4). Therefore, these YFP-Ace1 constructs all demonstrated significant specificity toward Cu^+.

To determine the affinity of our YFP-Ace1 probes to Cu^+, we monitored the response of our probes to a series of solutions in which the free Cu^+ concentration was buffered from 8.6×10^{-16} to 9.6×10^{-21} M. The response of YAG2 at each concentration was plotted, and a binding curve (Figure 2D) was generated. From the fitting of this curve, the K_d of YAG2 for Cu^+ was determined to be 8.2×10^{-18} M. The same titration was performed for each of the probes, and the range of K_d values varied from $\sim 10^{-18}$ to $\sim 10^{-19}$ M, depending on the length of the linker. The maximum response and K_d for each of the probes are summarized in Table 1. Each of these probes demonstrated a strong selectivity toward Cu^+. Longer linker lengths tended to improve the binding affinity (Table 1, Figure S7), creating a variety of probes that could have specific uses, depending on the level of labile copper ions.

***In Vivo* Characterization of YAG2.** To test the ability of our probes to monitor Cu^+ fluctuations in living systems, HeLa cells were transfected with a plasmid containing YAG2. All images were collected using a Leica SP2 laser scanning confocal microscope. The cells were monitored prior to addition of Cu^+, and then 50 μM $CuSO_4$ was added to the growth medium. The cells were monitored over several minutes, and the maximum fluorescence change occurred after only ~2 min. Interestingly, the addition of copper caused a decrease in the fluorescence intensity of our probes (Figure 5A–F), opposite to the response observed in our *in vitro* experiments. Addition of the known copper (I) chelator neocuprione (1 mM) caused an increase in the response (Figure 5G–I), which is again the reverse of the *in vitro* response. Addition of the possible competitor metal ion Zn^{2+} did not cause a signal response, and no response was observed upon the addition of EGTA, a common chelator for various metal ions (Figure 6). Further work is currently under way to identify the cause of this inverted response. Nevertheless, YAG2 demonstrated a remarkable capacity for monitoring Cu^+ fluctuations inside living cells, approaching 40% change of fluorescence upon copper addition.

Finally, to confirm that the signal change observed during imaging was a result of Cu^+ binding, the fluorescence responses in both *E. coli* and HeLa cells were also tested using fluorescence-activated cell sorting (FACS). When 500 nM $CuSO_4$ was added to the medium of *E. coli* cells followed by incubation for 30 min, a minor increase of the fluorescence signal was observed by FACS (Figure S8). As expected, when

dx.doi.org/10.1021/ja3106779 | *J. Am. Chem. Soc.* 2013, 135, 3144–3149

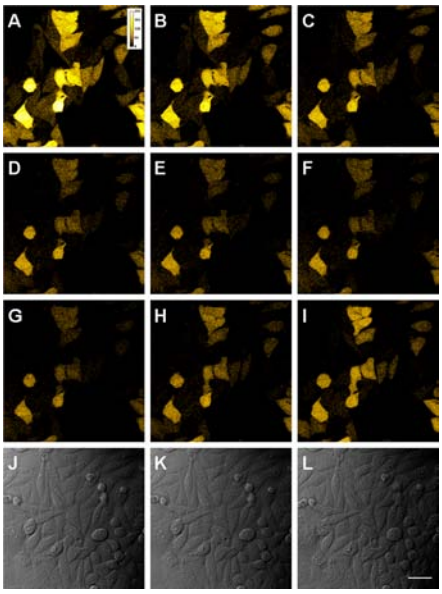

Figure 5. YAG2 response to incubation with Cu^+ in living HeLa cells. HeLa cells expressing YAG2 were incubated with 50 μM Cu^+ for (A) 0 s, (B) 30 s, (C) 1 min, (D) 2 min, (E) 3 min, and (F) 5 min. The fluorescence response showed a decrease over the first 2 min of Cu^+ incubation before leveling off and stabilizing. Subsequent to Cu^+ incubation, the known Cu^+ chelator neocuprione was added for (G) 0 min, (H) 10 min, and (I) 15 min. Longer incubation times with neocuprione proved capable of restoring much of the original fluorescence level. DIC images were captured (J) prior to analyte incubation, (K) after 5 min of Cu^+ incubation, and (L) after 15 min of neocuprione incubation to monitor cell physiology. Scale bar = 40 μm.

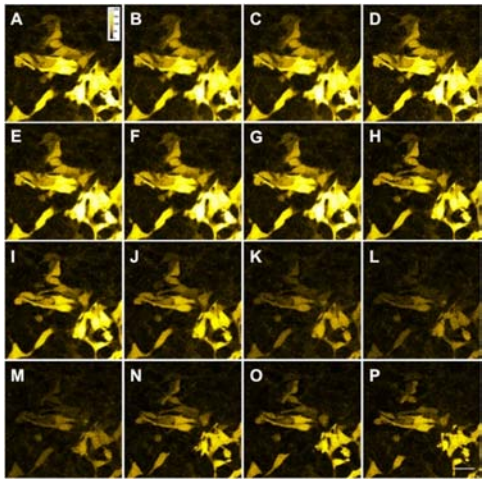

Figure 6. Response of YAG2 in HeLa cells. Cells were incubated with 100 μM zinc for (A) 0, (B) 1, (C) 2, or (D) 5 min and then imaged. The known metal ion chelator EGTA was then added to a final concentration of 1 mM, and cells were incubated for (E) 0, (F) 1, (G) 5, or (H) 10 min prior to imaging. Afterward, 50 μM copper(I) was added for (I) 0, (J) 1, (K) 2, or (L) 5 min before 1 mM neocuprione was added for (M) 0, (N) 1, (O) 5, or (P) 10 min. Scale bar = 40 μm.

neocuproine was added, the fluorescence response was decreased. Interestingly, this response was reversed when the experiment was performed in HeLa cells, consistent with what was observed from the imaging experiments. The FACS experiments thus support the conclusion that the signal change inside cells was indeed caused by Cu^+ binding with YFP-Ace1, whereas the fluorescence response was inverted in HeLa cells.

CONCLUSIONS

We have constructed a series of fluorescent reporters for Cu^+ by using the regulatory protein Ace1.[30,37] These new reporters demonstrate improved fluorescent responses *in vitro* and *in vivo*. Our newly constructed sensors also have varied binding affinities to Cu^+. These newly constructed genetically encoded Cu^+ reporters are currently being utilized to study copper homeostasis inside biological systems. The strategy employed could be further optimized in designing and developing genetically encoded probes for metal imaging and detection inside cells or even animals.

ASSOCIATED CONTENT

Supporting Information

Supporting Figures S1–S8. This material is available free of charge via the Internet at http://pubs.acs.org.

AUTHOR INFORMATION

Corresponding Author

chuanhe@uchicago.edu; pengchen@pku.edu.cn

Present Address

[#]Department of New Materials and Biosystems, Max-Planck-Institute for Intelligent Systems, Stuttgart 70569, Germany

Notes

The authors declare no competing financial interest.

ACKNOWLEDGMENTS

We thank C. Labno at the University of Chicago, BSD Microscopy Core Facilities, for help with the imaging experiments. This work was funded by research grants from the National Key Basic Research Program of China (2011CB809103), National Natural Science Foundation of China (21001010), and National Science Foundation CHE-1213598 (C.H.).

REFERENCES

(1) Robinson, N. J.; Winge, D. R. In *Annual Reviews in Biochemistry*, Vol. 79; Kornberg, R. D., Raetz, C. R. H., Rothman, J. E., Thorner, J. W., Eds.; Annual Reviews: Palo Alto, 2010; Vol. *79*, pp 537–562.
(2) Waldron, K. J.; Robinson, N. J. *Nat. Rev. Microbiol.* **2009**, *7*, 25–35.
(3) Huffman, D.; O'Halloran, T. V. *Annu. Rev. Biochem.* **2001**, *70*, 677–701.
(4) Changela, A.; Chen, K.; Xue, Y.; Holschen, J.; Outten, C. E.; O'Halloran, T. V.; Mondragon, A. *Science* **2003**, *301*, 1383–1387.
(5) Xiao, Z. G.; Loughlin, F.; George, G. N.; Howlett, G. J.; Wedd, A. G. *J. Am. Chem. Soc.* **2004**, *126*, 3081–3090.
(6) Dupont, C. L.; Grass, G.; Rensing, C. *Metallomics* **2011**, *3*, 1109–1118.
(7) Tiffany-Castiglioni, E.; Hong, S.; Qian, Y. C. *Int. J. Dev. Neurosci.* **2011**, *29*, 811–818.
(8) Kang, Y. J. *Pharmacol. Ther.* **2011**, *129*, 321–331.
(9) Madsen, E.; Gitlin, J. D. In *Annual Reviews in Neuroscience*; Annual Reviews: Palo Alto, 2007; Vol. *30*, pp 317–337.
(10) Zhang, X.; Kong, R.; Lu, Y. *Annu. Rev. Anal. Chem.* **2011**, *4*, 105–128.
(11) Hirayama, T.; Van de Bittner, G. C.; Gray, L. W.; Lutsenko, S.; Chang, C. J. *Proc. Natl. Acad. Sci. U.S.A.* **2012**, *109*, 2228–2233.
(12) Dodani, S. C.; Leary, S. C.; Cobine, P. A.; Winge, D. R.; Chang, C. J. *J. Am. Chem. Soc.* **2011**, *133*, 8606–8616.

(13) Dodani, S. C.; Domaille, D. W.; Nam, C. I.; Miller, E. W.; Finney, L. A.; Vogt, S.; Chang, C. J. *Proc. Natl. Acad. Sci. U.S.A.* **2011**, *108*, 5980−5985.
(14) Jung, H. S.; Kwon, P. S.; Lee, J. W.; Kim, J. I.; Hong, C. S.; Kim, J. W.; Yan, S. H.; Lee, J. Y.; Lee, J. H.; Joo, T.; Kim, J. S. *J. Am. Chem. Soc.* **2009**, *131*, 2008−2012.
(15) Zhao, Y.; Zhang, X. B.; Han, Z. X.; Qiao, L.; Li, C. Y.; Jian, L. X.; Shen, G. L.; Yu, R. Q. *Anal. Chem.* **2009**, *81*, 7022−7030.
(16) Que, E. L.; Gianolio, E.; Baker, S. L.; Wong, A. P.; Aime, S.; Chang, C. J. *J. Am. Chem. Soc.* **2009**, *131*, 8527−8536.
(17) Zhou, Z.; Fahrni, C. J. *J. Am. Chem. Soc.* **2004**, *126*, 8862−8863.
(18) Royzen, M.; Dai, Z. H.; Canary, J. W. *J. Am. Chem. Soc.* **2005**, *127*, 1612−1613.
(19) Brunner, J.; Kraemer, R. *J. Am. Chem. Soc.* **2004**, *126*, 13626−13627.
(20) Liu, J.; Lu, Y. *J. Am. Chem. Soc.* **2007**, *129*, 9838−9839.
(21) Miller, E. W.; Zeng, L.; Domaille, D. W.; Chang, C. J. *Nat. Protoc.* **2006**, *1*, 824−827.
(22) Zeng, L.; Miller, E. W.; Pralle, A.; Isacoff, E. Y.; Chang, C. J. *J. Am. Chem. Soc.* **2006**, *128*, 10−11.
(23) Grynkiewicz, G.; Poenie, M.; Tsien, R. Y. *J. Biol. Chem.* **1985**, *260*, 3440−3450.
(24) Miyawaki, A.; Tsien, R. Y. *Methods Enzymol.* **2000**, *327*, 472−500.
(25) Miyawaki, A.; Llopis, J.; Heim, R.; McCaffery, J. M.; Adams, J. A.; Ikura, M.; Tsien, R. Y. *Nature* **1997**, *388*, 882−887.
(26) Qin, Y.; Dittmer, P. J.; Park, J. G.; Jansen, K. B.; Palmer, A. E. *Proc. Natl. Acad. Sci. U.S.A.* **2011**, *108*, 7351−7356.
(27) Vinkenborg, J. L.; Nicolson, T. J.; Bellomo, E. A.; Koay, M. S.; Rutter, G. A.; Merkx, M. *Nat. Methods* **2009**, *6*, 737−740.
(28) Van Dongen, E.; Dekkers, L. M.; Spijker, K.; Meijer, E. W.; Klomp, L. W. J.; Merkx, M. *J. Am. Chem. Soc.* **2006**, *128*, 10754−10762.
(29) Qiao, W.; Mooney, M.; Bird, A. J.; Winge, D. R.; Eide, D. J. *Proc. Natl. Acad. Sci. U.S.A.* **2006**, *103*, 8674−8679.
(30) Wegner, S. V.; Arslan, H.; Sunbul, M.; Yin, J.; He, C. *J. Am. Chem. Soc.* **2010**, *132*, 2567−2569.
(31) Gralla, E. B.; Thiele, D. J.; Silar, P.; Valentine, J. S. *Proc. Natl. Acad. Sci. U.S.A.* **1991**, *88*, 8558−8562.
(32) Thorvaldsen, J. L.; Sewell, A. K.; Tanner, A. M.; Peltier, J. M.; Pickering, I. J.; George, G. N.; Winge, D. R. *Biochemistry* **1994**, *33*, 9566−9577.
(33) Dobi, A.; Dameron, C. T.; Hu, S.; Hamer, D.; Winge, D. R. *J. Biol. Chem.* **1995**, *270*, 10171−10178.
(34) Dameron, C. T.; Winge, D. R.; George, G. N.; Sansone, M.; Hu, S.; Hamer, D. *Proc. Natl. Acad. Sci. U.S.A.* **1991**, *88*, 6127−6131.
(35) Graden, J. A.; Posewitz, M. C.; Simon, J. R.; George, G. N.; Pickering, I. J.; Winge, D. R. *Biochemistry* **1996**, *35*, 14583−14589.
(36) Evers, T. H.; van Dongen, E.; Faesen, A. C.; Meijer, E. W.; Merkx, M. *Biochemistry* **2006**, *45*, 13183−13192.
(37) Wegner, S. V.; Sun, F.; Hernandez, N.; He, C. *Chem Commun.* **2011**, *47*, 2571−2573.